

25 making them easier to fast-track to clinical studies in COVID-19 patients. Here, we present data
26 on the antiviral activity of 20 FDA approved drugs against SARS-CoV-2 that also inhibit SARS-
27 CoV and MERS-CoV. We found that 17 of these inhibit SARS-CoV-2 at a range of IC50 values
28 at non-cytotoxic concentrations. We directly follow up with seven of these to demonstrate all are
29 capable of inhibiting infectious SARS-CoV-2 production. Moreover, we have evaluated two of
30 these, chloroquine and chlorpromazine, *in vivo* using a mouse-adapted SARS-CoV model and
31 found both drugs protect mice from clinical disease.

32

33 **Introduction**

34 At the end of December 2019, reports started to emerge from China of patients suffering from
35 pneumonia of unknown etiology. By early January, a new coronavirus had been identified and
36 determined as the cause (1). Since then, the virus originally known as novel coronavirus 2019
37 (nCoV-2019), now severe acute respiratory syndrome coronavirus 2 (SARS-CoV-2), has spread
38 around the world. As of April 23th, 2020, there have been roughly 2.7 million confirmed cases of
39 COVID-19 (the disease caused by SARS-CoV-2 infection) with over to 189,000 recorded deaths
40 (www.WHO.org). Multiple countries have enacted social distancing and quarantine measures,
41 attempting to reduce person-to-person transmission of the virus. Healthcare providers lack
42 pharmaceutical countermeasures against SARS-CoV-2, beyond public health interventions, and
43 there remains a desperate need for rapid development of antiviral therapeutics. A potential route
44 to candidate antivirals is through repurposing of already approved drugs (for reviews; (2–4) and
45 for examples;(5–8). We have previously screened a library of FDA approved drugs for antiviral
46 activity against two other highly pathogenic human coronaviruses, SARS-CoV and Middle East
47 respiratory syndrome coronavirus (MERS-CoV)(6). We found 27 drugs that inhibited replication
48 of both of these coronaviruses, suggesting that they may have broad anti-coronaviral activity.
49 One of the hits from this work was imatinib with which we subsequently determined the

50 mechanism of action by demonstrating this drug inhibits fusion of coronaviruses with cellular
51 membranes, thus blocking entry (9, 10).

52

53 Here, we present our investigation of 20 priority compounds from our previous screening to test
54 if they can also inhibit SARS-CoV-2. Since these compounds are already approved for use in
55 humans, they make ideal candidates for drug repurposing and rapid development as antiviral
56 therapeutics. Our work found that 17 of the 20 of the drugs that inhibited SARS-CoV and
57 MERS-CoV could also inhibit SARS-CoV-2, with similar IC₅₀ values. We further assessed a
58 subset of these drugs for their effects on SARS-CoV-2 RNA and infectious virus production and
59 found all to have inhibitory activity. Our screening based on cytopathic effect therefore appears
60 a favorable approach to find drugs capable of inhibiting production of infectious virus. Currently
61 there are no established small animal model systems for SARS-CoV-2. However, there is a
62 well-established mouse-adapted system for SARS-CoV (MA15 strain(11)) and we present data
63 here assessing the *in vivo* efficacy of chloroquine (CQ) and chlorpromazine (CPZ) against
64 SARS-CoV. We found that drug treatment does not inhibit virus replication in mouse lungs, but
65 significantly improves clinical outcome. Based on both of these drugs inhibiting SARS-CoV-2
66 infection *in vitro* and providing protection *in vivo* against SARS-CoV clinical disease we believe
67 they may be beneficial for SARS-CoV-2 therapy, but require further study in clinical contexts.

68

69 **Materials and Methods**

70 **Cell lines and virus**

71 Vero E6 cells (ATCC# CRL 1586) were cultured in DMEM (Quality Biological), supplemented
72 with 10% (v/v) fetal bovine serum (Sigma), 1% (v/v) penicillin/streptomycin (Gemini Bio-
73 products) and 1% (v/v) L-glutamine (2 mM final concentration, Gibco). Cells were maintained at
74 37°C and 5% CO₂. Samples of SARS-CoV-2 were obtained from the CDC following isolation

75 from a patient in Washington State (WA-1 strain - BEI #NR-52281). Stocks were prepared by
76 infection of Vero E6 cells for two days when CPE was starting to be visible. Media were
77 collected and clarified by centrifugation prior to being aliquoted for storage at -80°C. Titer of
78 stock was determined by plaque assay using Vero E6 cells as described previously (12). All
79 work with infectious virus was performed in a Biosafety Level 3 laboratory and approved by our
80 Institutional Biosafety Committee. SARS-CoV stock was prepared as previously described (13).
81 SARS-CoV spike (S) pseudotype viruses were produced as previously described (9).

82

83 **Drug testing**

84 All drug screens were performed with Vero E6 cells. Cells were plated in opaque 96 well plates
85 one day prior to infection. Drug stocks were made in either DMSO, water or methanol. Drugs
86 were diluted from stock to 50 µM and an 8-point 1:2 dilution series made. Cells were pre-treated
87 with drug for 2 hour (h) at 37°C/5% CO₂ prior to infection at MOI 0.01 or 0.004. Vehicle controls
88 were used on every plate, and all treatments were performed in triplicate for each screen. In
89 addition to plates that were infected, parallel plates were left uninfected to monitor cytotoxicity of
90 drug alone. Three independent screens with this set-up were performed. Cells were incubated
91 at 37°C/5% CO₂ for 3 days before performing CellTiter-Glo (CTG) assays as per the
92 manufacturer's instruction (Promega). Luminescence was read using a Molecular Devices
93 Spectramax L plate reader. Fluphenazine dihydrochloride, benztropine mesylate, amodiaquine
94 hydrochloride, amodiaquine dihydrochloride dihydrate, thiethylperazine maleate, mefloquine
95 hydrochloride, triparanol, terconazole vetranal, anisomycin, fluspirilene, clomipramine
96 hydrochloride, hydroxychloroquine sulfate, promethazine hydrochloride, emetine dihydrochloride
97 hydrate and chloroquine phosphate were all purchased from Sigma. Chlorpromazine
98 hydrochloride, toremifene citrate, tamoxifen citrate, gemcitabine hydrochloride and imatinib
99 mesylate were all purchased from Fisher Scientific.

100

101 **Data analysis**

102 Cytotoxicity (%TOX) data was normalized according to cell-only uninfected (cell only) controls
103 and CTG-media-only (blank) controls:

$$\%TOX = \left(1 - \frac{(drug) - (blank)}{(cell\ only) - (blank)} \right) \times 100$$

104 Inhibition (%Inhibit) data was normalized according to cell only and the activity of the vehicle
105 controls:

$$\%Inhibit = \frac{(drug) - (vehicle)}{(cell\ only) - (vehicle)} \times 100$$

106 Nonlinear regression analysis was performed on the normalized %inhibit and %TOX data and
107 IC50s and CC50s were calculated from fitted curves (log [agonist] versus response - variable
108 slope [four parameters]) (GraphPad Software, LaJolla, CA), as described previously (14). Drug
109 dilution points in a given run were excluded from IC50 analysis if the average cytotoxicity was
110 greater than 30% (arbitrary cutoff) across the 3 cytotoxicity replicates for that screen. IC50 or
111 CC50 values extrapolated outside the drug dilution range tested were reported as greater than
112 50µM or less than 0.39µM. Selectivity indexes (SI) were also calculated by dividing the CC50 by
113 the IC50.

114

115 **Viral infection**

116 To further analyse candidate drugs, Vero E6 cells were grown in 24 well plate format for 24 h
117 prior to infection. As with the drug screens, cells were pre-treated with drug at a range of
118 concentrations, or vehicle control for 2 h. Cells were then infected with SARS-CoV-2 at MOI 0.1
119 for 24 hour (h). Supernatant was collected, centrifuged in a table-top centrifuge for 3 minutes
120 (min) at max speed and stored at -80°C. After a wash in PBS, infected cells were collected in

121 TRIZol (Ambion) for RNA analysis (described below). Supernatant was used to titer viral
122 production by TCID₅₀ assay (12).

123

124 **RNA extraction and qRT-PCR**

125 RNA was extracted from TRIZol samples using Direct-zol RNA miniprep kit (Zymo Research) as
126 per the manufacturer's instructions. RNA was converted to cDNA using RevertAid RT Kit
127 (Thermo Scientific), with 12 µl of extracted RNA per reaction. For qRT-PCR, 2 µl of cDNA
128 reaction product was mixed with PowerUp SYBR Green Master Mix (Applied Biosystems) and
129 WHO/Corman primers targeting N and RdRp: N FWD 5'-CACATTGGCACCCGCAATC-3', N
130 REV 5'-GAGGAACGAGAAGAGGCTTG-3', RdRp FWD 5'GTGARATGGTCATGTGTGGCGG-
131 3', RdRp REV 5'-CARATGTTAAASACACTATTAGCATA-3'. The qRT-PCR reactions were
132 performed with a QuantStudio 5 (Applied Biosystems). To normalize loading, 18S RNA was
133 used as a control, assessed with TaqMan Gene Expression Assays (Applied Biosystems) and
134 TaqMan Fast Advanced Master Mix. Fold change between drug treated and vehicle control was
135 determined by calculating $\Delta\Delta CT$ after normalization to the endogenous control of 18S.

136

137

138 **Pseudovirus fusion/entry assay**

139 The pseudovirion (PV) entry assay was performed as described (9, 15). Briefly, 2×10^4 BSC1
140 cells per well were in 96-well plates for 24 h, after which time cells were pre-treated with drug (1
141 h) and infected with PV (3 h). Media was removed and cells were washed with loading buffer
142 (47 ml clear DMEM, 5 mM Probenecid, 2 mM L-glutamine, 25 mM HEPES, 200 nM bafilomycin,
143 5 µM E64D) and incubated for 1 h in CCF2 solution (LB, CCF2-AM, Solution B [CCF2-AM kit
144 K1032] Thermo Fisher) in the dark. Cells were washed once with loading buffer and incubated
145 from 6 h to overnight with 10% FBS in loading buffer. Percentage CCF2 cleavage was assessed

146 by flow cytometry on the LSRII (Beckton Dickinson) in the flow cytometry core facility at the
147 University of Maryland, Baltimore. Data were analyzed using FlowJo.

148

149 **Mouse infections.**

150 All infections were performed in an animal biosafety level 3 facility at the University of Maryland,
151 Baltimore, using appropriate practices, including a HEPA-filtered bCON caging system, HEPA-
152 filtered powered air-purifying respirators (PAPRs), and Tyvek suiting. All animals were grown to
153 10 weeks of age prior to use in experiments. The animals were anesthetized using a mixture of
154 xylazine (0.38 mg/mouse) and ketamine (1.3 mg/mouse) in a 50 μ l total volume by
155 intraperitoneal injection. The mice were inoculated intranasally with 50 μ l of either PBS or 2.5 x
156 10^3 PFU of rMA15 SARS-CoV (11) after which all animals were monitored daily for weight loss.
157 Mice were euthanized at day 4 post-infection, and lung tissue was harvested for further
158 analysis. All animals were housed and used in accordance with the University of Maryland,
159 Baltimore, Institutional Animal Care and Use Committee guidelines.

160

161 **Plaque assay.**

162 Vero cells were seeded in 35 mm dishes with 5×10^5 cells per dish 24 h prior to
163 infection. Supernatants from homogenized were serially diluted 10^{-1} through 10^{-6} in serum-free
164 (SF) media. Cells were washed with SF media, 200 μ l of diluted virus was added to each well
165 and adsorption was allowed to proceed for 1 h at 37°C with gentle rocking every 10 min. 2X
166 DMEM and 1.6% agarose were mixed 1:1. Cells were washed with SF media, 2 ml DMEM-
167 agarose was added to each well, and cells were incubated for 72 h at 37°C, after which time
168 plaques were read.

169

170

171 **Results**

172 **Screening FDA approved compounds for anti-SARS-CoV-2 activity**

173 Previously, we performed a large-scale drug screen on 290 FDA approved compounds to
174 investigate which may have antiviral activity against SARS-CoV and MERS-CoV (6). With the
175 emergence of SARS-CoV-2, we prioritized testing 20 of the 27 hits that were determined to
176 inhibit both of the previously tested coronaviruses for antiviral activity against the novel virus.
177 The list of tested compounds is shown in Table 1. Our screening started at 50 μ M and used an
178 8-point, 1:2 dilution series with infections being performed at either MOI 0.01 or 0.004. CellTiter-
179 Glo (CTG) assays were performed 3 days post-infection to determine relative cell viability
180 between drug and vehicle control treated cells. Uninfected samples were used to measure the
181 cytotoxicity of drug alone. From the relative luminescence data of the CTG assay, percent
182 inhibition (of cell death caused by viral infection) could be measured and plotted along with the
183 percent cytotoxicity of drug alone. Fig. 1 shows these plotted graphs from one representative of
184 three independent screens at MOI 0.01. For those drugs demonstrating a cell toxicity rate lower
185 than 30%, we were able to calculate IC₅₀ values at both MOI from these graphs for 17 of the 20
186 drugs which is summarized in Table 1.

187

188 **Drug screen validation**

189 In order to validate our screening process as a means to identify compounds with antiviral effect
190 we decided to follow up with a subset of drugs. Chloroquine (CQ) has become the source of
191 much interest as a potential treatment for COVID19 (16), as such, we further investigated
192 hydroxychloroquine (HCQ) and CQ as both were present in our screen (Table 1). Vero E6 cells
193 were plated and pre-treated with drug for 2 h prior to infection with SARS-CoV-2 at MOI 0.1.
194 Supernatant was collected 24 h post-infection to determine titer of virus by TCID₅₀ assay and
195 cells were collected in TRIzol to assess production of viral mRNA. Treatment with both drugs
196 caused a significant reduction in viral mRNA levels, especially at higher concentrations, without
197 drug induced cytotoxicity (Fig. 1 and Table 1). There was a significant decrease in relative

198 expression levels of both RdRp and N mRNA across the range of concentrations used (Fig. 2A-
199 D). Along with causing a reduction in viral mRNA, treatment with both drugs caused a significant
200 reduction in viral replication (Fig. 2E and 2F). SARS-CoV-2 production was more sensitive to
201 HCQ than CQ with larger inhibition seen at the same concentration of treatment, which is in
202 agreement with HCQ having a lower IC₅₀ in our cell viability assay (Table 1). We also
203 performed a time of addition assay with the highest concentration of HCQ to investigate whether
204 SARS-CoV-2 entry was the point of inhibition of this compound (Fig. 2G). Interestingly, while the
205 addition of HCQ at 2h post-infection did have some reduction in inhibitory activity there was not
206 a complete loss, suggesting that HCQ treatment may impact other stages of the viral life cycle
207 than just entry.

208

209 We have previously used a β -lactamase-Vpr chimeric protein (Vpr-BlaM) pseudotype system to
210 demonstrate that imatinib (a drug also seen to inhibit SARS-CoV-2 [Table 1 and Fig. 1]) inhibits
211 SARS-CoV and MERS-CoV spike-mediated entry (9). We used this system to more directly
212 investigate whether CQ could inhibit viral entry mediated by coronavirus spike, and additionally
213 included chlorpromazine (CPZ) as this is known to inhibit clathrin-mediated endocytosis (17)
214 and was also part of our drug screening (Table 1 and Fig. 2). In this assay, when the
215 pseudovirus fuses with a cellular membrane, BlaM is released into the cytoplasm of the infected
216 cell. BlaM cleaves cytoplasmic loaded CCF2 to change its emission spectrum from 520 nm
217 (green) to ~450 nm (blue), which can be quantified using flow cytometry.

218

219 Cells were treated with CQ or CPZ for 1 h before infection with BlaM-containing SARS-S
220 pseudovirions (PV). Cells were then analyzed by flow cytometry to quantify the cleavage of
221 CCF2. In mock treated cells infected with SARS-S PV there was a shift in the CCF2 emission
222 spectrum indicating release of BlaM to the cytosol, and that spike-mediated fusion with cellular
223 had occurred. Upon treatment with CQ or CPZ there was a greater than 90% reduction in CCF2

224 cleavage caused by SARS-S PV (Fig. 2H). These data demonstrate that both drugs inhibit
225 SARS-CoV spike-mediated fusion with cellular membranes. These pseudotype assays suggest
226 that the inhibition of coronavirus replication caused by CQ and CPZ is at the stage of entry to
227 cells but combined with the time of addition assays (Fig. 2G), there is a suggestion that later
228 stages may also be impacted.

229
230 HCQ and CQ are used as anti-malarial drugs and are in the class of aminoquinolines which are
231 hemozoin inhibitors, similarly to 4-methanolquinolines. Interestingly, from our drug screening,
232 three other hemozoin inhibitors were identified: amodiaquine dihydrochloride dihydrate,
233 amodiaquine hydrochloride and mefloquine. We therefore decided to directly test these drugs
234 for antiviral activity against SARS-CoV-2. We directly tested CPZ against SARS-CoV-2 having
235 seen that it could inhibit SARS-CoV S-mediated entry to cells (Fig. 2H). We also included
236 imatinib since we have previously shown that this can inhibit entry of both SARS-CoV and
237 MERS-CoV (9) and was a hit against SARS-CoV-2 (Fig. 1 and Table 1). Again, cells were pre-
238 treated with drugs at the indicated concentrations and infected with SARS-CoV-2 at MOI 0.1 for
239 24h, after which supernatant samples were collected. As can be seen in Fig. 3, at the highest
240 concentrations of all drugs there is significant inhibition of SARS-CoV-2 infection. All five drugs
241 showed very strong inhibition at 20 μ M.

242
243 Overall, the data from Fig. 2 and Fig. 3 indicate that there are various FDA approved drugs that
244 have broad-spectrum anti-coronavirus activity *in vitro* and that our initial screening based on
245 cytopathic effect is a good method to identify compounds with antiviral activity.

246
247 **Chloroquine and chlorpromazine do not inhibit SARS-CoV (MA15) replication in mouse**
248 **lungs, but significantly reduces weight loss and clinical signs**

249 CQ and CPZ treatment displayed significant inhibition of coronavirus replication *in vitro*, with our
250 data suggesting entry is inhibited. We therefore decided to investigate whether these drugs
251 were efficacious *in vivo* using SARS-CoV strain, MA15 in BALB/c mice. This model displays
252 ~15-20% weight loss by 4 days post infection (dpi), occasionally resulting in death. We tested
253 whether prophylactically administered CQ or CPZ could protect mice from severe MA15
254 infection. Mice were injected intraperitoneally with either water, 0.8 mg CQ, 1.6 mg CQ, 20 µg
255 CPZ, 100 µg CPZ or 200 µg CPZ at day -1 of infection and then were dosed every day through
256 the 4 days of infection. On day 0, mice were intranasally infected with 2.5×10^3 pfu of SARS-
257 CoV (MA15) or PBS as control. Weight loss was measured as a correlate of disease and mice
258 were euthanized at 4 dpi for analysis.

259
260 PBS inoculated mice showed no weight loss or clinical signs of disease when treated with either
261 water, CQ or CPZ over the experiment time course indicating drug treatment did not adversely
262 affect morbidity (Fig. 4A and 4D). Mice that were infected with MA15 and treated with water lost
263 ~15% of their starting body weight over 4 days and had significant clinical signs of disease
264 including ruffled fur, labored breathing and lethargy (Fig. 4A and 4D). Mice that were treated
265 with 0.8 mg of CQ each day, displayed similar weight loss as the water control through the first
266 3 days of infection, however by 4 dpi the weight loss was halted in the drug treated mice (Fig.
267 4A). Mice that were treated with 1.6 mg CQ per day showed markedly reduced weight loss
268 compared to the water control (Fig. 4A). Pathological analysis was also performed on H&E
269 stained sections. Mice infected with MA15 and treated with water displayed significant
270 inflammation and denuding bronchiolitis suggesting severe disease (Fig. 4B). By contrast, 0.8
271 mg CQ dose group had moderate inflammation that was reduced compared to control and the
272 1.6 mg dose group had minimal lung pathology (Fig. 4B). Interestingly, even though CQ
273 treatment appeared to protect against weight loss and inflammation in the lungs, the viral titer
274 was equivalent between drug treated and vehicle control mice (Fig. 4C).

275
276 Similar to the CQ results, CPZ treatment reduced weight loss in mice infected with MA15 at 100
277 μg and 200 μg , but the 20 μg treatment group were equivalent to vehicle control (Fig. 4D) and
278 the H&E sections showed protection against inflammation and denuding bronchiolitis at the
279 higher doses (Fig. 4E). Again, as with CQ treatment, even though there were reduced signs of
280 infection with CPZ treatment, there was no difference in MA15 titer in the mouse lungs (Fig. 4F).
281 Overall these data indicate that even though CQ and CPZ treatment do not inhibit viral
282 replication in the lungs, both can protect mice from signs of disease following SARS-CoV
283 (MA15) infection.

284

285 **Discussion**

286 The SARS-CoV-2 pandemic has demonstrated the desperate need for antiviral drugs. Since the
287 emergence of SARS-CoV in 2002, research has uncovered many details of coronavirus biology
288 and pathogenesis, however there are currently no approved therapeutics against this emerging
289 virus family. Whether being used for treating SARS-CoV-2 in this current pandemic or the next
290 unknown viral pathogen in the future, we must attempt to develop and validated antiviral drugs
291 that are ready to be used at the first signs of an outbreak. Many FDA approved drugs have been
292 found to have antiviral activity in addition to their approved use (e.g; (5–8)), and since these are
293 extensively used in humans for other conditions, they could be streamlined for rapid approval
294 and repositioning as antivirals. In our previous work, 290 FDA approved drugs were screened
295 for antiviral activity and 27 were found to inhibit both SARS-CoV and MERS-CoV (6). We
296 prioritized testing these for antiviral activity against SARS-CoV-2 since they displayed broad-
297 spectrum antiviral activity. From multiple independent screens performed with two MOI, we
298 found that 17 of our 20 tested priority compounds display significant antiviral activity at non-
299 cytotoxic concentrations. Many of the compounds have IC₅₀ values under 10 μM and these will
300 be the source of follow up testing on additional cell lines and in mouse models of SARS-CoV-2.

301

302 We further investigated seven of the hits to directly test if they inhibited SARS-CoV-2 replication.

303 We performed follow-up experiments with HCQ, CQ, amodiaquine and mefloquine because

304 chloroquine has garnered much interest as a potential treatment for COVID19 (16) and the

305 others are similarly used as anti-malarial compounds (18). In addition, we have previously

306 demonstrated that imatinib is an inhibitor of SARS-CoV, MERS-CoV and infectious bronchitis

307 virus entry to cells (9, 10) so included that here as the mechanism of coronavirus inhibition is

308 understood. Finally, CPZ inhibits clathrin function in cells (17) so can disrupt infection by many

309 viruses that require clathrin-mediated endocytosis and was therefore also chosen for further

310 analysis. Treatment of cells with all these drugs showed inhibition of infectious viral particle

311 production (measured by TCID₅₀ assay) at non-cytotoxic levels.

312

313 Having demonstrated that HCQ, CQ and CPZ can inhibit cytopathic effect, mRNA synthesis and

314 infectious viral particle production of SARS-CoV-2, we used a previously published system of

315 SARS-CoV pseudotype viruses carrying Vpr-BlaM to investigate whether CQ and CPZ inhibit

316 coronavirus spike-mediated entry to better define mechanism of action. We have previously

317 used this system to define imatinib as an entry inhibitor of these viruses (9) and found similar

318 results for CQ and CPZ, thus better defining their mechanism of antiviral activity.

319

320 Finally, we investigated the efficacy of CQ and CPZ with an *in vivo* model using SARS-CoV

321 MA15. There is currently a lack of an established mouse model for SARS-CoV-2 so we used the

322 mouse adapted SARS-CoV (MA15) strain as a surrogate to assess the *in vivo* efficacy of these

323 drugs against a closely related coronavirus. We are of the opinion that this is a good model

324 since both viruses use ACE2 as a receptor (19–22) and therefore have a similar cellular tropism

325 which is important since both of these compounds appear to inhibit viral entry. Prophylactic

326 dosing in MA15 infection experiments demonstrated that, in contrast to the *in vitro* antiviral

327 activity, CQ and CPZ did not inhibit viral replication in mouse lungs based on viral titer
328 recovered from lungs at 4 dpi. However, both drugs resulted in reduced weight loss and
329 improved clinical outcome, with the higher dose giving greater protection. Along with being an
330 anti-malarial, CQ is used in humans for the treatment of systemic lupus erythematosus and
331 rheumatoid arthritis because of anti-inflammatory properties and has effects on antigen
332 presentation (23–25). We speculate that these properties may have a role in the protection we
333 observe *in vivo* since much of the pathology from SARS-CoV is a consequence of
334 immunopathology during infection (in mice; (26), in non-human primates (27) and for a detail
335 review (28)). These results suggest that CQ alone may not be a viable therapeutic but may be
336 beneficial for treatment of SARS-CoV-2 in combination with more directly acting antivirals such
337 as remdesivir (29–31).

338
339 The development of antiviral drugs for emerging coronaviruses is a global priority. In the middle
340 of the COVID19 pandemic, we must identify rapidly accessible therapeutics that are validated in
341 both *in vitro* and *in vivo* models. FDA approved drugs being assessed for repurposing and other
342 experimental drugs in development must be properly validated in animal studies to best assess
343 their potential utility in people. We have presented here a list of FDA approved drugs that are
344 effective *in vitro* against SARS-CoV-2 as well as being effective against SARS-CoV and MERS-
345 CoV (6). Moreover, we have demonstrated that two of these, CQ and CPZ, can protect mice
346 from severe clinical disease from SARS-CoV. Future research will be aimed at testing these
347 compounds in SARS-CoV-2 animal models to further assess their potential utility for human
348 treatment.

349

350 **Acknowledgments**

351 We kindly thank Emergent BioSolutions for financial support to perform these experiments. We
352 also kindly thank Julie Dyall for helpful discussions regarding data analysis.

353

354 **References**

- 355 1. Zhu N, Zhang D, Wang W, Li X, Yang B, Song J, Zhao X, Huang B, Shi W, Lu R, Niu P,
356 Zhan F, Ma X, Wang D, Xu W, Wu G, Gao GF, Tan W. 2020. A novel coronavirus from
357 patients with pneumonia in China, 2019. *N Engl J Med* 382:727–733.
- 358 2. Sisk JM, Frieman MB. 2016. Screening of FDA-Approved Drugs for Treatment of
359 Emerging Pathogens. *ACS Infect Dis*. American Chemical Society.
- 360 3. Pushpakom S, Iorio F, Eyers PA, Escott KJ, Hopper S, Wells A, Doig A, Guilliams T,
361 Latimer J, McNamee C, Norris A, Sanseau P, Cavalla D, Pirmohamed M. 2018. Drug
362 repurposing: Progress, challenges and recommendations. *Nat Rev Drug Discov*.
- 363 4. Mercorelli B, Palù G, Loregian A. 2018. Drug Repurposing for Viral Infectious Diseases:
364 How Far Are We? *Trends Microbiol* 26:865–876.
- 365 5. Madrid PB, Chopra S, Manger ID, Gilfillan L, Keepers TR, Shurtleff AC, Green CE, Iyer L
366 V., Dilks HH, Davey RA, Kolokoltsov AA, Carrion R, Patterson JL, Bavari S, Panchal RG,
367 Warren TK, Wells JB, Moos WH, Burke RLL, Tanga MJ. 2013. A Systematic Screen of
368 FDA-Approved Drugs for Inhibitors of Biological Threat Agents. *PLoS One* 8.
- 369 6. Dyall J, Coleman CM, Hart BJ, Venkataraman T, Holbrook MR, Kindrachuk J, Johnson
370 RF, Olinger GG, Jahrling PB, Laidlaw M, Johansen LM, Lear-rooney CM, Glass PJ,
371 Hensley LE, Frieman B. 2014. Repurposing of Clinically Developed Drugs for Treatment
372 of Middle East Respiratory Syndrome Coronavirus Infection. *Antimicrob Agents*
373 *Chemother* 58:4885–4893.
- 374 7. Madrid PB, Panchal RG, Warren TK, Shurtleff AC, Endsley AN, Green CE, Kolokoltsov A,
375 Davey R, Manger ID, Gilfillan L, Bavari S, Tanga MJ. 2016. Evaluation of Ebola Virus
376 Inhibitors for Drug Repurposing. *ACS Infect Dis* 1:317–326.
- 377 8. Xu M, Lee EM, Wen Z, Cheng Y, Huang WK, Qian X, Tcw J, Kouznetsova J, Ogden SC,
378 Hammack C, Jacob F, Nguyen HN, Itkin M, Hanna C, Shinn P, Allen C, Michael SG,

- 379 Simeonov A, Huang W, Christian KM, Goate A, Brennand KJ, Huang R, Xia M, Ming GL,
380 Zheng W, Song H, Tang H. 2016. Identification of small-molecule inhibitors of Zika virus
381 infection and induced neural cell death via a drug repurposing screen. *Nat Med* 22:1101–
382 1107.
- 383 9. Coleman CM, Sisk JM, Mingo RM, Nelson EA, White JM, Frieman MB. 2016. Abl Kinase
384 Inhibitors Are Potent Inhibitors of SARS-CoV and MERS-CoV Fusion. *J Virol* 90:8924–
385 8933.
- 386 10. Sisk JM, Frieman MB, Machamer CE. 2018. Coronavirus S protein-induced fusion is
387 blocked prior to hemifusion by Abl kinase inhibitors. *J Gen Virol* 1–12.
- 388 11. Roberts A, Deming D, Paddock CD, Cheng A, Yount B, Vogel L, Herman BD, Sheahan T,
389 Heise M, Genrich GL, Zaki SR, Baric R, Subbarao K. 2007. A mouse-adapted SARS-
390 coronavirus causes disease and mortality in BALB/c mice. *PLoS Pathog* 3:0023–0037.
- 391 12. Coleman CM, Frieman MB. 2015. Growth and Quantification of MERS-CoV Infection.
392 *Curr Protoc Microbiol* 37:15E.2.1-15E.2.9.
- 393 13. Frieman M, Yount B, Agnihothram S, Page C, Donaldson E, Roberts A, Vogel L,
394 Woodruff B, Scorpio D, Subbarao K, Baric RS. 2012. Molecular Determinants of Severe
395 Acute Respiratory Syndrome Coronavirus Pathogenesis and Virulence in Young and
396 Aged Mouse Models of Human Disease. *J Virol* 86:884–897.
- 397 14. Dyall J, Johnson JC, Hart BJ, Postnikova E, Cong Y, Zhou H, Gerhardt DM, Michelotti J,
398 Honko AN, Kern S, DeWald LE, O’Loughlin KG, Green CE, Mirsalis JC, Bennett RS,
399 Olinger GG, Jahrling PB, Hensley LE. 2018. In Vitro and In Vivo Activity of Amiodarone
400 Against Ebola Virus. *J Infect Dis* 218:S592–S596.
- 401 15. Mingo RM, Simmons JA, Shoemaker CJ, Nelson EA, Schornberg KL, D’Souza RS,
402 Casanova JE, White JM. 2015. Ebola Virus and Severe Acute Respiratory Syndrome
403 Coronavirus Display Late Cell Entry Kinetics: Evidence that Transport to NPC1 +
404 Endolysosomes Is a Rate-Defining Step. *J Virol* 89:2931–2943.

- 405 16. Pastick KA, Okafor EC, Wang F, Lofgren SM, Skipper CP, Nicol MR, Pullen MF,
406 Rajasingham R, Mcdonald EG, Lee TC, Schwartz IS, Kelly LE, Lothar SA, Mitjà O,
407 Letang E, Abassi M, Boulware DR. 2020. Review: Hydroxychloroquine and Chloroquine
408 for Treatment of SARS-CoV-2 (COVID-19). *Open Forum Infect Dis*.
- 409 17. Wang LH, Rothberg KG, Anderson RGW. 1993. Mis-assembly of clathrin lattices on
410 endosomes reveals a regulatory switch for coated pit formation. *J Cell Biol* 123:1107–
411 1117.
- 412 18. Baird JK. 2005. Effectiveness of antimalarial drugs. *N Engl J Med* 352.
- 413 19. Li W, Moore MJ, Vasllieva N, Sui J, Wong SK, Berne MA, Somasundaran M, Sullivan JL,
414 Luzuriaga K, Greeneugh TC, Choe H, Farzan M. 2003. Angiotensin-converting enzyme 2
415 is a functional receptor for the SARS coronavirus. *Nature* 426:450–454.
- 416 20. Zhou P, Yang X Lou, Wang XG, Hu B, Zhang L, Zhang W, Si HR, Zhu Y, Li B, Huang CL,
417 Chen HD, Chen J, Luo Y, Guo H, Jiang R Di, Liu MQ, Chen Y, Shen XR, Wang X, Zheng
418 XS, Zhao K, Chen QJ, Deng F, Liu LL, Yan B, Zhan FX, Wang YY, Xiao GF, Shi ZL.
419 2020. A pneumonia outbreak associated with a new coronavirus of probable bat origin.
420 *Nature* 579:270–273.
- 421 21. Wan Y, Shang J, Graham R, Baric RS, Li F. 2020. Receptor Recognition by the Novel
422 Coronavirus from Wuhan: an Analysis Based on Decade-Long Structural Studies of
423 SARS Coronavirus. *J Virol* 94.
- 424 22. Hoffmann M, Kleine-Weber H, Schroeder S, Krüger N, Herrler T, Erichsen S, Schiergens
425 TS, Herrler G, Wu NH, Nitsche A, Müller MA, Drosten C, Pöhlmann S. 2020. SARS-CoV-
426 2 Cell Entry Depends on ACE2 and TMPRSS2 and Is Blocked by a Clinically Proven
427 Protease Inhibitor. *Cell* 181:271-280.e8.
- 428 23. Ziegler HK, Unanue ER. 1982. Decrease in macrophage antigen catabolism caused by
429 ammonia and chloroquine is associated with inhibition of antigen presentation to T cells.
430 *Proc Natl Acad Sci U S A* 79:175–178.

- 431 24. Al-Bari MAA. 2015. Chloroquine analogues in drug discovery: new directions of uses,
432 mechanisms of actions and toxic manifestations from malaria to multifarious diseases. *J*
433 *Antimicrob Chemother* 70:1608–21.
- 434 25. Rainsford KD, Parke AL, Clifford-Rashotte M, Kean WF. 2015. Therapy and
435 pharmacological properties of hydroxychloroquine and chloroquine in treatment of
436 systemic lupus erythematosus, rheumatoid arthritis and related diseases.
437 *Inflammopharmacology* 23:231–269.
- 438 26. Rockx B, Baas T, Zornetzer GA, Haagmans B, Sheahan T, Frieman M, Dyer MD, Teal
439 TH, Proll S, van den Brand J, Baric R, Katze MG. 2009. Early Upregulation of Acute
440 Respiratory Distress Syndrome-Associated Cytokines Promotes Lethal Disease in an
441 Aged-Mouse Model of Severe Acute Respiratory Syndrome Coronavirus Infection. *J Virol*
442 83:7062–7074.
- 443 27. Smits SL, De Lang A, Van Den Brand JMA, Leijten LM, Van Ijcken WF, Eijkemans MJC,
444 Van Amerongen G, Kuiken T, Andeweg AC, Osterhaus ADME, Haagmans BL. 2010.
445 Exacerbated innate host response to SARS-CoV in aged non-human primates. *PLoS*
446 *Pathog* 6.
- 447 28. Channappanavar R, Perlman S. 2017. Pathogenic human coronavirus infections: causes
448 and consequences of cytokine storm and immunopathology. *Semin Immunopathol*
449 39:529–539.
- 450 29. Wang M, Cao R, Zhang L, Yang X, Liu J, Xu M, Shi Z, Hu Z, Zhong W, Xiao G. 2020.
451 Remdesivir and chloroquine effectively inhibit the recently emerged novel coronavirus
452 (2019-nCoV) in vitro. *Cell Res* 0.
- 453 30. Brown AJ, Won JJ, Graham RL, Dinnon KH, Sims AC, Feng JY, Cihlar T, Denison MR,
454 Baric RS, Sheahan TP. 2019. Broad spectrum antiviral remdesivir inhibits human
455 endemic and zoonotic deltacoronaviruses with a highly divergent RNA dependent RNA
456 polymerase. *Antiviral Res* 169.

457 31. Sheahan TP, Sims AC, Graham RL, Menachery VD, Gralinski LE, Case JB, Leist SR,
458 Pirc K, Feng JY, Trantcheva I, Bannister R, Park Y, Babusis D, Clarke MO, MacKman
459 RL, Spahn JE, Palmiotti CA, Siegel D, Ray AS, Cihlar T, Jordan R, Denison MR, Baric
460 RS. 2017. Broad-spectrum antiviral GS-5734 inhibits both epidemic and zoonotic
461 coronaviruses. *Sci Transl Med* 9.

462

463

464

465 **Figure legend**

466 **Figure 1 – Percentage inhibition and percentage cytotoxicity graphs from drug screens**
467 **starting at 50 μ M using an 8-point, 1:2 dilution series.** Results from one representative drug
468 screen of three showing percentage inhibition and cytotoxicity for each of the tested drugs.
469 Triplicate wells of cells were pre-treated with the indicated drug for 2 hours prior to infection with
470 SARS-CoV-2 at MOI 0.01. Cells were incubated for 72 hours prior to performing CellTiter-Glo
471 assays to assess cytopathic effect. Data are scored as percentage inhibition of relative cell
472 viability for drug treated versus vehicle control. Data are the mean percentages with error bars
473 displaying standard deviation between the triplicate wells.

474

475 **Figure 2 – Hydroxychloroquine and chloroquine inhibit production of SARS-CoV-2 N and**
476 **RdRp mRNA.**

477 Vero cells were pre-treated with hydroxychloroquine sulfate (A, C and E) or chloroquine
478 phosphate (B, D and F) at the indicated concentration (or 0.1% water as vehicle control) for 2 h
479 prior to infection with SARS-CoV-2 (WA-1 strain) at MOI 0.1. 24 h post-infection cells were
480 collected in TRIzol. RNA was extracted from TRIzol sample and qRT-PCR was performed for
481 viral RdRp (A and B) or N (C and D) mRNA using WHO primers. RNA levels were normalized
482 with 18S RNA and fold change for drug treated to vehicle control was calculated (dotted line to

483 denote a fold change of 1 which is no change over control). Data are from 3 independent
484 infections performed on triplicate wells, the fold change was calculated in each independent
485 experiment and the mean fold change is plotted with error bars displaying standard deviation.
486 Along with TRIzol samples for RNA supernatant was collected from cells and used for TCID₅₀
487 assays to determine infectious virus production following treatment with HCQ (E) or CQ (F) Data
488 are from 3 independent infections performed on triplicate wells with the TCID₅₀/ml being
489 averaged across all wells. Error bars are the standard deviation. G) Cells were treated with 50
490 µM HCQ or 0.1% water as control. Drug was either added 2 h prior to infection, at the time of
491 infection or 2 h after infection with MOI 0.1 SARS-CoV-2. After 24 h infection, supernatant was
492 collected and used for TCID₅₀ assays to determine infectious virus production. Data are from 3
493 independent infections performed on triplicate wells with the TCID₅₀/ml being averaged across
494 all wells. Error bars are the standard deviation. H) SARS-CoV spike psuedoviruses (PV) were
495 used for infection of BSC1 cells. The cells were treated with 10 µM of CQ or CPZ for 1 h prior to
496 infection with PV for 3 h. The PV carry BlaM and cells were loaded with CCF2 to monitor
497 cleavage and shift in fluorescence output for evidence of S-mediated entry into cells. Data are
498 normalised to PV alone and are from 3 independent experiments with error bars representing
499 standard deviation.

500

501 **Figure 3 – Antiviral activity of additional FDA approved compounds against SARS-CoV-2.**

502 Other drugs that showed antiviral activity in our initial CellTiter-Glo screening were tested for
503 inhibition of productive virus infection. Cells were treated with the indicated concentrations of A)
504 amodiaquine dihydrochloride dihydrate, B) amodiaquine hydrochloride, C) chlorpromazine, D)
505 mefloquine and E) imatinib for 2 h prior to infection with SARS-CoV-2 at MOI 0.1 for 24 h.
506 Supernatant was collected and used for TCID₅₀ assay to quantify infectious virus production.
507 Data are from a representative experiment of four performed on triplicate wells. Data are the
508 mean TCID₅₀/ml with error bars being standard deviation.

509

510 **Figure 4 – CQ and CPZ are protective against SARS-CoV (MA15) infection *in vivo***

511 Mice were treated with CQ or CPZ 1 day prior to infection with SARS-CoV (MA15) and dosed
512 with each drug across the 4 day infection time course. Water was used as the vehicle control for
513 both drugs and PBS was used as a control for uninfected mice. A) Weight loss of mice treated
514 with CQ at two different dose levels (0.8 mg and 1.6 mg) over the 4 day infection. Data are
515 presented as relative weight loss compared to the mouse weight on day 0. In each treatment
516 group there were 5 mice and the data are mean average and standard deviation. B) At day 4,
517 mice were euthanized and lung sections were used for H&E staining. C) In addition to collecting
518 lungs for section staining, there was also collection to determine titer of virus by plaque assay.
519 D) Weight loss of mice treated with CPZ at three different doses (20 µg, 100 µg, and 200 µg)
520 with the same experimental set up as in A. E and F) As B and C but for CPZ treated mice.

521

522 **Table 1 - IC50 and CC50 values for 20 FDA approved drugs against SARS-CoV-2.**

523 Abbreviations: MOI (multiplicity of infection), IC50 (half maximal inhibitory concentration), CC50
524 (half maximal cytotoxic concentration), avg. (average), ND (not determined).

525 A – Run totals listed as IC50,CC50

526 B – At least one CC50 could be extrapolated from the curve fit suggesting toxicity and SI are
527 slightly higher than listed

528 C – No CC50 could be extrapolated from the curve fit suggesting toxicity and SI are much
529 higher than listed.

530

531

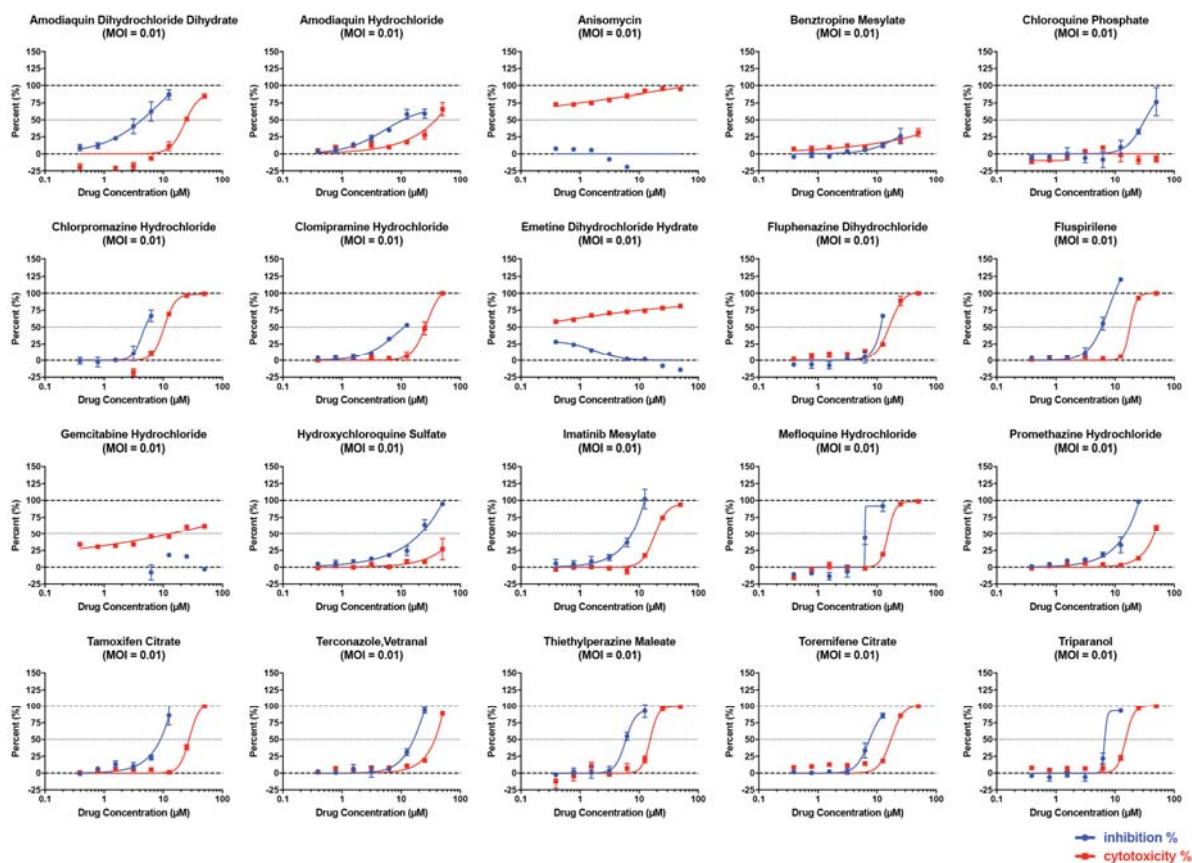
532

533

534

535
536
537
538
539
540
541
542

Figure 1



543
544
545
546
547

548

549

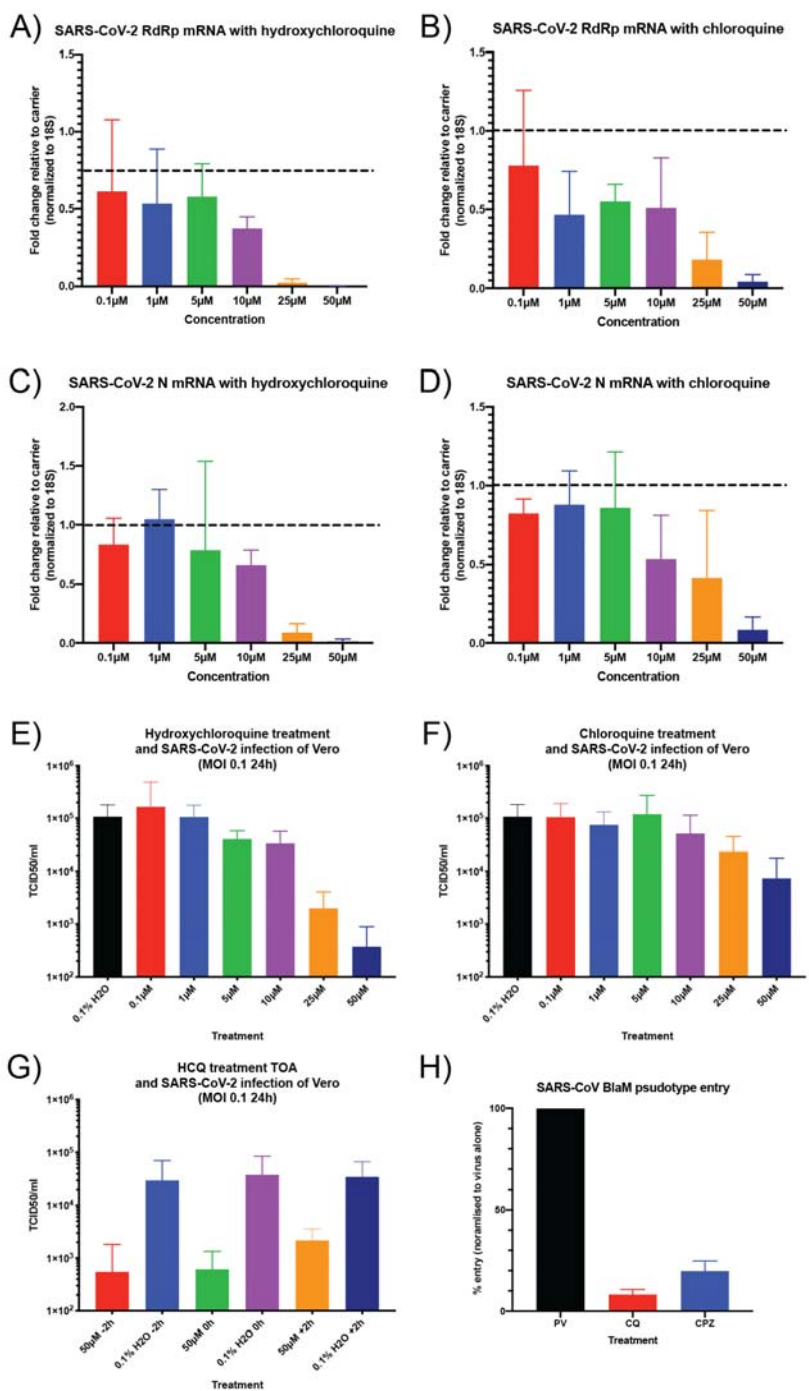
550

551

552

553

554 **Figure 2**



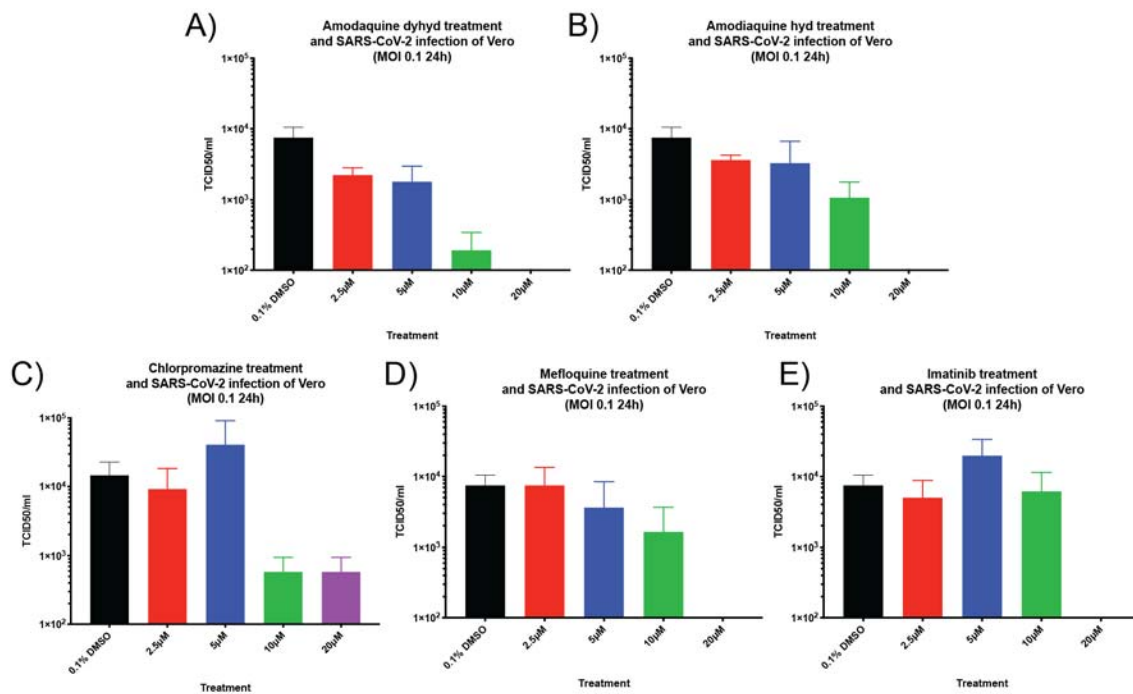
555

556

557

558

559 **Figure 3**



560

561

562

563

564

565

566

567

568

569

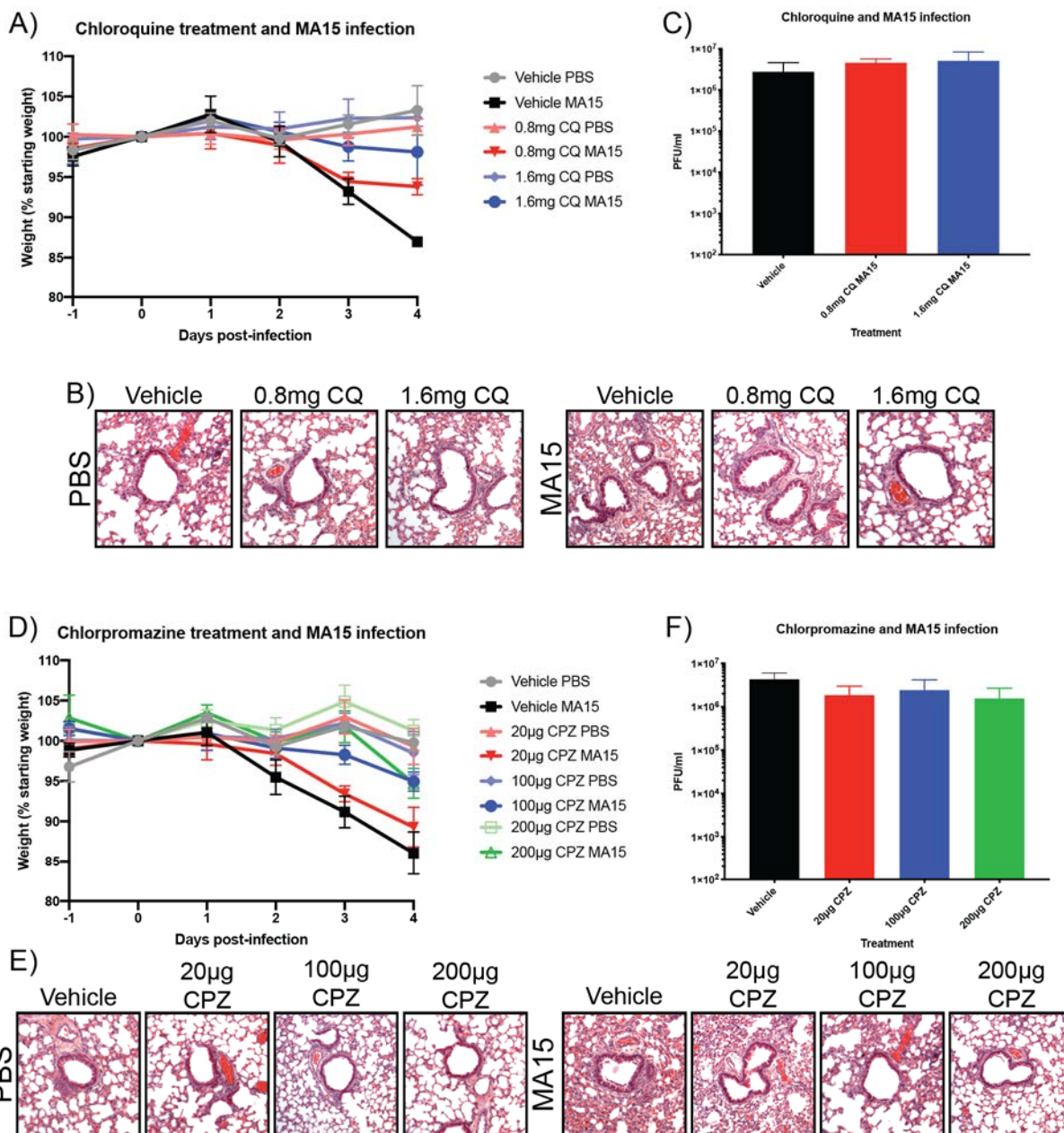
570

571

572

573

574 **Figure 4**



575

576

577

578

579

580

581 **Table 1**

Drug	MOI	Plate Replicates	IC50 (avg.)	CC50 (avg.)	SI (avg.)
Amodiaquine Dihydrochloride Dihydrate	0.004	2,3 ^a	2.59	34.42	13.31
	0.01	3	4.94	34.42	6.97
Amodiaquine Hydrochloride	0.004	3	2.36	>38.63 ^b	>16.37 ^b
	0.01	3	5.64	>38.63 ^b	>6.84 ^b
Anisomycin	0.004	3	ND	<0.39	ND
	0.01	3	ND	<0.39	ND
Benztropine Mesylate	0.004	3	13.8	>>50 ^c	>>3.62 ^c
	0.01	2,3 ^a	17.79	>>50 ^c	>>2.81 ^c
Chloroquine Phosphate	0.004	3	42.03	>50 ^b	>1.19 ^b
	0.01	3	46.8	>50 ^b	>1.07 ^b
Chlorpromazine Hydrochloride	0.004	2,3 ^a	3.14	11.88	3.78
	0.01	2,3 ^a	4.03	11.88	2.94
Clomipramine Hydrochloride	0.004	2,3 ^a	5.63	>29.68 ^b	>5.27 ^b
	0.01	3	7.59	>29.68 ^b	>3.91 ^b
Emetine Dihydrochloride Hydrate	0.004	3	ND	<0.39	ND
	0.01	2,3 ^a	ND	<0.39	ND
Fluphenazine Dihydrochloride	0.004	3,2 ^a	6.36	20.02	3.15
	0.01	2	8.98	20.02	2.23
Fluspirilene	0.004	3	3.16	30.33	9.61
	0.01	3	5.32	30.33	5.71
Gemcitabine Hydrochloride	0.004	3	ND	23.22	ND
	0.01	3	ND	23.22	ND
Hydroxychloroquine Sulfate	0.004	3	9.21	>>50 ^c	>>5.43 ^c
	0.01	3	11.17	>>50 ^c	>>4.48 ^c
Imatinib Mesylate	0.004	3	3.24	>30.86 ^b	>9.52 ^b
	0.01	3	5.32	>30.86 ^b	>5.80 ^b
Mefloquine Hydrochloride	0.004	3	7.11	18.53	2.61
	0.01	3	8.06	18.53	2.3
Promethazine Hydrochloride	0.004	3	9.21	>42.59 ^b	>4.62 ^b
	0.01	3	10.44	>42.59 ^b	>4.08 ^b
Tamoxifen Citrate	0.004	2	34.12	37.96	1.11
	0.01	1,2 ^a	8.98	37.96	4.23
Terconazole Vetrinal	0.004	3	11.92	41.46	3.48
	0.01	2,3 ^a	16.14	41.46	2.57
Thiethylperazine Maleate	0.004	3	7.09	18.37	2.59
	0.01	3	8.02	18.37	2.29
Toremifene Citrate	0.004	2,3 ^a	4.77	20.51	4.3
	0.01	3	11.3	20.51	1.81
Triparanol	0.004	2,3 ^a	4.68	21.21	4.53
	0.01	2,3 ^a	6.41	21.21	3.31

582

583